Resonance tube phonation in water – the effect of tube diameter and water depth on back pressure and bubble characteristics at different airflows

Wistbacka, Greta

Amaranta Andrade, Pedro

Simberg, Susanna

Hammarberg, Britta

Södersten, Maria

Svec, Jan

Granqvist, Svante

Abstract:

Resonance tube phonation with tube end in water is a voice therapy method in which the patient phonates through a glass tube keeping the free end of the tube submerged into water, creating bubbles.

Objectives: The purpose of this experimental study was to determine flow-pressure relationship, flow thresholds between bubble types and bubble frequency as function of flow and back volume.

Methods: A flow driven vocal tract simulator was used for recording the back pressure produced by resonance tubes with inner diameters 8 and 9 mm submerged at water depths 0-7 centimeters. Visual inspection of bubble types through video recording was also performed.

Results: The static back pressure was largely determined by the water depth. The narrower tube provided a slightly higher back pressure for a given flow and depth. The amplitude of the pressure oscillations increased with flow and depth. Depending on flow, the bubbles were emitted from the tube in three distinct types with increasing flow; one by one, pairwise and in a chaotic manner. The bubble frequency was slightly higher for the narrower tube. An increase in back volume led to a decrease in bubble frequency.

Conclusions: This study provides data on physical properties of resonance tube phonation with tube end in water. This information will be useful in future research when looking into the possible effects of this type of voice training.

1. INTRODUCTION

Semi-occluded vocal tract (SOVT) exercises have a long history in voice training. Semi-occlusions can be accomplished via lip trills, tongue trills, raspberries, the hand-over-mouth technique or phonation into differently sized tubes with the free end kept in air or in water. Common for all these exercises is that they provide a flow resistance, leading to an increase in oral pressure and a decrease in transglottal pressure [1,2,3].

Resonance tube phonation in water is an exercise in which the user phonates into a glass tube keeping the free end of the tube submerged a few centimeters into a bowl of water [4]. This method provides an increase in oral pressure that fluctuates due to the water bubbles [5, 6, 7]. Clinicians have reported good clinical results using this method when treating patients with different kinds of voice disorders, such as vocal nodules, hyper- and hypofunction and vocal fold paresis [4, 8], and positive immediate effects have been reported in dysphonic patients [9] and healthy singers [5].

The developer of the method, Antti Sovijärvi [4], claimed that the tubes should have specific dimensions depending on the patient's voice category and age. He recommended tubes between 26 and 28 cm in length with a diameter of 9 mm for adults. Tubes for children should be between 24 and 26 cm in length with a diameter of 8 mm [4]. These recommendations are still taken into consideration in clinical practice [8], although there is, to our knowledge, no scientific evidence for why these specific tube dimensions would be more appropriate than others.

Amarante Andrade et al [10] investigated the pressure-flow relationship for different tube dimensions used in voice exercises. The results showed that a change in diameter affects the flow resistance to a greater extent than a corresponding relative change in length. The typical resonance tube diameter of 9 mm [4] generated a relatively low flow resistance for a given

flow, compared to narrower diameters of e.g. 3.3 mm or 6 mm. Later, Smith and Titze [11] conducted a similar study with the end of the tubes in free air, resulting in a model for the pressure-flow relationship, based on flow theory and empirical data. Submerging the tube into water adds another pressure component affecting the back pressure (p_{back}). When in water, the flow will not start until the pressure given by the water depth has been overcome [10].

In the clinical setting, Simberg and Laine [8] suggest three different versions of the resonance tube in water exercise depending on the aim of the training. For treating for example hyperfunction or vocal nodules, they recommend continuous phonation while keeping the tube end submerged 1-2 cm into the water. For treating patients with insufficient vocal fold closure, they recommend short phonations while keeping the tube end submerged as deep as 15 cm into the water, resembling pushing exercises. For treating e.g. hypofunction, they recommend continuous phonation while keeping the tube end close to the water surface, with the end of the tube partially open. A similar voice training method is the LaxVox technique, in which continuous phonation through a silicone tube submerged into a water bottle is used [12]. The water depths recommended in this technique are 1–7 cm, hence deeper than in the resonance tube method.

When the tube end is submerged into water during continuous phonation, the bubbles cause oscillation in the oral pressure [5,6,7,10]. Patients using this version of the method have referred to the sensation in the throat as "*relaxing, like a 'massage'*" [8], and the oscillations in the oral pressure have later been referred to as implementing a "massage-effect" in the larynx [2,5,7,13,14]. However, it remains unclear exactly what constitutes this presumed effect.

Little systematic examination of bubble formation and frequency for resonance tube phonation in water has been done. Ramlakhan, Mudde, Oosterbaan-Beks, Goes-de Graaff and Arendse [15] used high-speed imaging to visually observe bubble formations during

resonance tube phonation in water, suggesting that bubbles exit the tube in a steady but alternating pattern followed by a back flow of water into the tube. Further, there are some reports on bubble frequencies with human participants without measurement of flow [6,7,13,16]. However, the effect of flow on the formation of bubbles in water and other fluids with upward facing orifices were examined already in the 1950's by Davidson and Amick [17] among others. They found that for low flows, the bubble size was almost independent of flow, and thus the bubble frequency was proportional to the flow. For higher flows, the bubble size increased with flow, and the bubble frequency plateaued at a maximum rate. Also, they found that the volume of the cavity behind the tube inlet affected the bubble size and frequency. For certain flows they also observed bimodally (pairwise) emitted bubbles, forming the shape of a mushroom. Tufaile and Sartorelli [18] also observed doublets of bubbles being formed from upward facing orifices, but in a mixture of water and glycerin. For higher flows they observed quadruplets and chaotic behavior in the formation of bubbles.

During resonance tube phonation in water, the static and oscillating parts of p_{back} directly affect the vocal apparatus [5,6,7,16]. Apart from this, the bubbles might play an important role providing visual, auditory and tactile feedback for the clinician and patient during the exercise. The purpose of the present study was to investigate characteristics of p_{back} and bubbles generated by glass tubes submerged into water. The tubes were connected to a flow-driven vocal tract simulator with a variable back cavity volume. The simulator provided a continuous airflow to resemble the exercises with continuous phonation described by Simberg and Laine [8].

2. METHOD

2.1 Setup

A flow-driven vocal tract simulator was used, consisting of a pressurized air cylinder, connected via a mass flow controller (Alicat Scientific model MCR-50SLPM-TFT), to a 60 ml syringe providing a cavity with an adjustable size and an outlet for tube connection. A differential pressure transducer, 8-SOP MPXV7007DP-ND, Freescale Semiconductor, Petaling Jaya Malaysia was attached to the syringe, see Figure 1. Calibration of pressure was performed by means of a U-tube manometer.
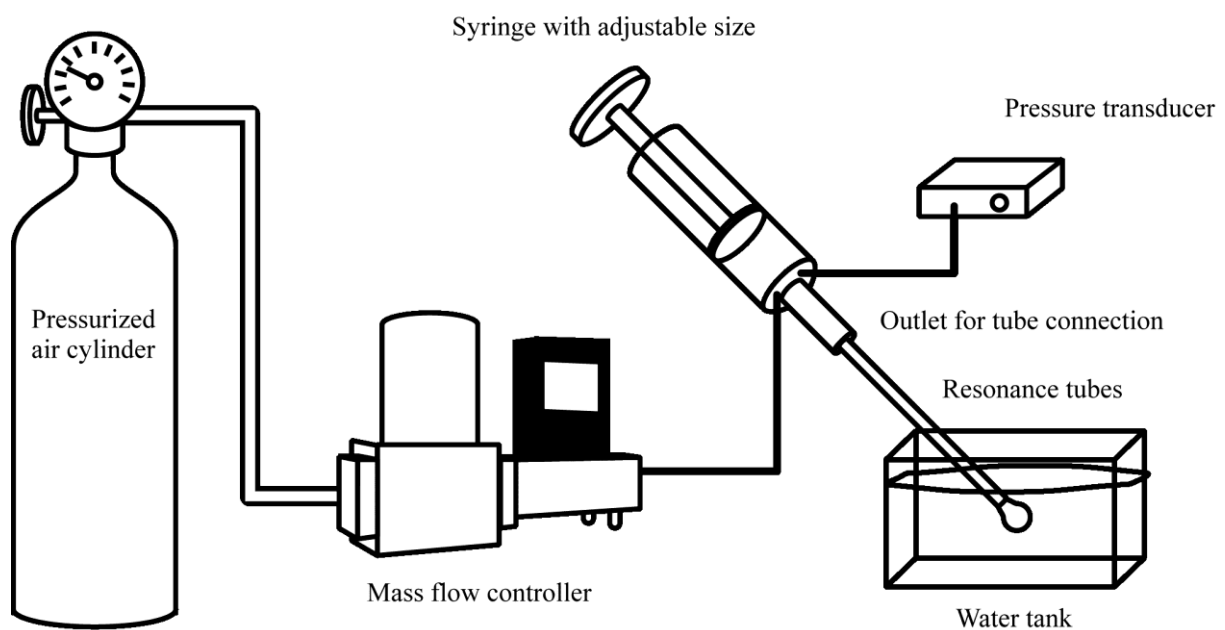

Figure 1. The airflow-driven vocal tract simulator.

The pressure in the back cavity, the flow signal from the flow controller and the audio were recorded using the Soundswell Signal Workstation for Windows version 4.00 build 4003 with an analogue library SwellDSP 4.00 and DSP card LSI PC/C32 (Neovius Data och signalsystem AB, www.neovius.se). The channels were recorded at a sampling rate of 16 kHz each. The audio signal was used for logging purposes only. For measurements requiring a varying flow, a custom written software Mjau was used to control the flow controller. Some recordings were supplemented with video filming, using a Canon 700D model (Canon inc., www.canon.com)

at a rate of 50 frames per second, exposure time 1/1000 s. The data analyses were made using the Sopran software version 1.0.12 (Tolvan Data, www.tolvan.com) and Matlab version R2015b (Mathworks inc. www.mathworks.com). Statistical analyses were made using IBM SPSS Statistics 24 for Windows.

2.2 Materials

Two glass tubes with inner diameters Ø 8.0 and Ø 9.0 mm, glass thickness 1.0 mm and length 26 cm were used [4]. In the clinical setting, patients are instructed to keep a good, relaxed posture avoiding bending the neck or lowering the chin [8]. Based on these posture recommendations, the tubes in the present study were submerged into the water at a 45˚ angle, which should be an accurate estimate of the angle patients use in the clinical setting. All water depths were measured from the surface to the lowest part of the tube end, see figure 2.The size of the bowl used in the experiments was 165 x 105 x 95 mm. In experiments 1-4 the back volume of the syringe was set to 36 cm^3 in order to approximate the volume of the vocal tract [19]. The same angle of tube submersion as well as back volume were used in a previous study investigating p_{back} for different sized tubes with the free end in air and in water [10].
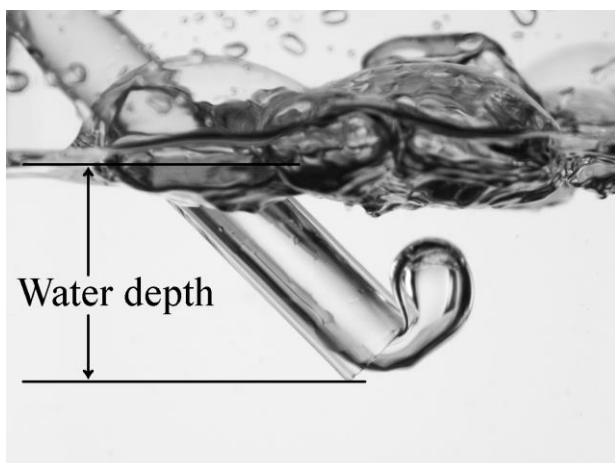

Figure 2. The definition of water depth used in this study

2.3 Experiments

2.3.1 Experiment 1, pressure as a function of flow.

The two tubes were assessed in air and at 7 different water depths (1-7 cm), to measure p_{back} as a function of flow. The flow was increased from 0 up to 0.38 L/s by the control software during 65 s. The static and oscillating components were analyzed separately.

Static component: The flow and pressure signals were resampled to 5 Hz in Sopran (this procedure automatically included low-pass filtering at 2.5 Hz to avoid aliasing effects) and exported to Matlab. In order to prepare the graphs, flow and pressure were further smoothed in Matlab using a 4 second moving average window.

For comparison, curves describing theoretical estimations were added. Based on the findings by Amarante Andrade et al [10], a combined model for the p_{back} was formulated:

$$p_{back} = p_{water} + p_{tube} \tag{1}$$

where p_{water} is the water pressure at the tube end and p_{tube} is the pressure determined by the flow through the tube and the tube resistance. The p_{tube} was modelled by the modified flow model presented by Smith and Titze [11]:

$$p_{tube} = \left(3.7631 \cdot 10^{-7} \cdot \frac{L}{D^{4.4997}} + 1.0268 \cdot 10^{-6} \cdot \frac{1}{D^{4.0416}}\right) U^2 + \left(3.9913 \cdot 10^{-9} \cdot \frac{L}{D^{5.0089}} + \right.$$
$$\left. 8.0169 \cdot 10^{-7} \cdot \frac{1}{D^{3.7696}}\right) U \tag{2}$$

where p_{tube} is the flow-dependent back pressure from the tube in free air in Pa, D is the tube diameter in m, U is the flow in L/s and L is the length of the tube in m.

Oscillating component: The pressure signal was processed in Sopran by high pass filtering at 1 Hz to remove the static component, extracting the root of the mean of the squares (RMS) from the filtered pressure signal using a smoothing filter cutoff at 0.3 Hz. The flow and RMS-pressure signals were resampled to 5 Hz and exported to Matlab.

6

In order to prepare the graphs, flow, pressure and RMS-pressure were further smoothed in Matlab using a 4 second moving average window.

2.3.2 Experiment 2, bubble types, video recording.

The Ø 9 mm tube was submerged at depths 2, 4 and 6 cm. Initial tests were conducted to visually identify different bubble patterns – regular, bimodal and chaotic. Based on these findings, video recordings were made during a slowly increasing flow. From these recordings, three flows (0.005, 0.013 and 0.050 L/s) were selected and consecutive images were extracted from the video recordings in order to illustrate the bubble types. The periodicity of p_{back} was analyzed by means of a correlogram using a window length of 50 ms. The correlogram is a method originally developed for analysis of voices with a high amount of perturbation in the fundamental frequency, using the correlation between two time windows of the signal. A correlogram shows time on the x-axis, time between windows on the y-axis and correlation coefficient on the z-axis displayed as a grey scale in a similar manner as in a spectrogram. Different candidates for period times appear as horizontal dark stripes. For a detailed description of correlograms, see Granqvist and Hammarberg [20].

2.3.3 Experiment 3, bubble types as function of flow.

To identify the flow thresholds between the different bubble patterns, the two tubes were submerged into water at depths 2, 4 and 6 cm. For each depth 10 recordings were made while the flow increased from 0 to 0.08 L/s during 70 s. This range of flow was determined by the initial tests to be sufficient for covering the thresholds between the investigated bubble types. The shifts between bubble formation modes were determined by visual inspection of correlograms by authors GW and SG. All conditions were rated twice by both raters to obtain intra rater reliability. Four shifts were determined, see figure 3. The first shift appeared when the first candidate started to deviate while the second candidate remained stable. The second

shift appeared when the first candidate was clearly divided in two. The third shift appeared when the separation in the first candidate became less clear and the second candidate started to become less stable, and the fourth shift appeared when no stable first and second candidates were visible. Flows at the shifts were noted for analyses, giving four flow threshold values for all takes: regular - regular with bimodal components - bimodal - bimodal with chaotic components -chaotic. Averages and standard deviations were calculated. Inter and intra rater reliability were calculated using intra class correlation (ICC) on the entire data sets. Differences in flow values at different shifts were analyzed using non-parametric statistics with regards to diameters and water depths.
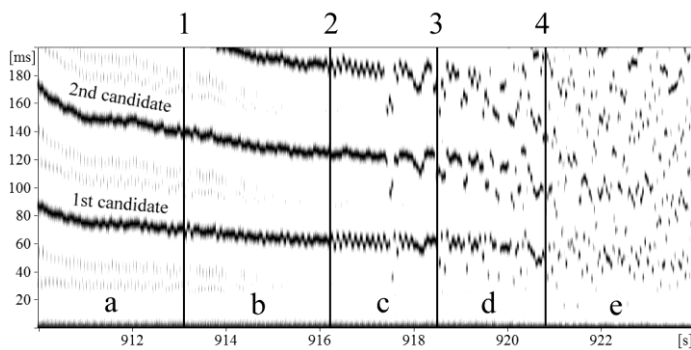

Figure 3. Correlogram analysis of the back pressure signal from a tube Ø 9 mm, length 26 cm, submerged 2 cm in water. The airflow is increasing from 0.001 to 0.07 L/s, left to right. The letters represent the different bubble modes: a) regular, b) regular with bimodal components, c) bimodal, d) bimodal with chaotic components and e) chaotic. The lines show the visual detection of shifts from (1) regular to regular with bimodal components, (2) regular with bimodal components to bimodal, (3) bimodal to bimodal with chaotic components and (4) chaotic. Back cavity volume was 36 cm^3 and angle of tube submersion 45°.

2.3.4 Experiment 4, bubble frequency and volume as functions of flow

The two tubes were submerged into water depths at 2, 4 and 6 cm. The flow was set to eleven different values between 0 and 0.04 L/s and kept steady in intervals of about 10 seconds. This reduced flow range was determined based on the results of experiment 3. All conditions were recorded 12 times. The bubble frequency was measured for each steady interval using a spectrum of the p_{back} signal over 4 seconds. The bubble frequencies were extracted for the cases when the bubbles were emitted regularly or bimodally. In the bimodal region the second spectral peak was extracted for analysis, i.e. the frequency reflects the actual number of bubbles per second, not the number of bubble pairs per second. Flows generating chaotic bubble patterns did not result in clear peaks in the spectra, therefore no measurements of bubble frequency were made for these flows.

The bubble volume was calculated by dividing the flow by the bubble frequency:

$$V = \frac{U}{f} \tag{3}$$

Where V is the volume of a bubble in L, U is the flow in L/s and f is the bubble frequency in Hz. Empirical mathematical models to describe the relation between flow and bubble frequency/volume were determined using the trendline function of Microsoft Office Excel. The power function resulted in the highest correlation coefficient.

2.3.5 Experiment 5, bubble frequency and volume as functions of back cavity volume

The two tubes were submerged into 2 cm water depth. Each tube was recorded using two fixed flows of 0.005 and 0.02 L/s while the volume of the back cavity was changed in intervals of about 10 seconds. Ten different volumes were set, ranging from 6 ml to 60 ml in steps of 6 ml. All conditions were recorded ten times. Bubble frequency and volume were measured as in experiment 4. Differences in bubble frequencies and volumes between back volumes and tube diameters were analyzed using non-parametric statistics.

3. RESULTS

3.1 Experiment 1, pressure/flow relationship

The static component of the pressure – flow relationship can be seen in figure 4. When the tube ends were kept in air, the p_{back} increased slightly with increasing flow. When the tube ends were kept in water, the p_{back} needed to reach a pressure near the corresponding water depth (as it is defined in this paper) before the flow could start. Further increase of the flow resulted in a slightly increased p_{back}. The shapes of the curves for different depths were similar, but shifted upwards by an amount approximately corresponding to the water depth. For very low flows, the required pressure occasionally was slightly lower than the corresponding water depth. The p_{back} from the Ø 8 mm tube increased slightly more with flow than from the Ø 9 mm tube.

The predictions for pressure-flow theory for tubes in air by Smith and Titze [11], provided a good match to the pressures for the tubes in free air. Our combined model predicts the p_{back} of the tube in water with a slight underestimation.
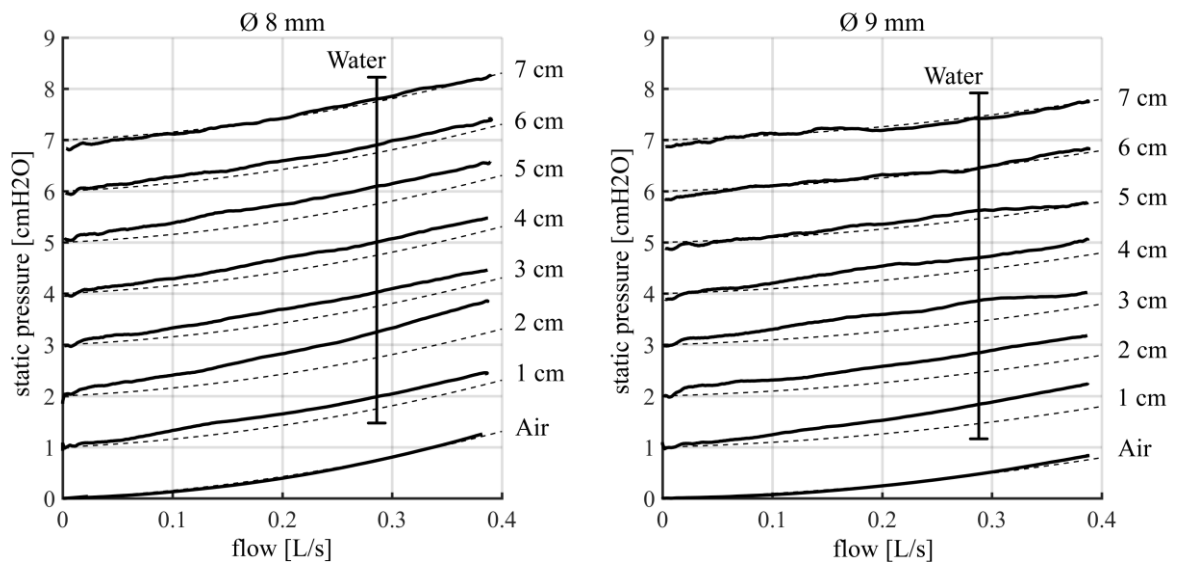

Figure 4. The flow-pressure relationship for resonance tubes, Ø 8 mm (left) and Ø 9 mm

(right), 26 cm length, in air and 1-7 cm of water depth. The back cavity volume was 36 cm^3 and angle of tube submersion 45°. The dashed lines represent our combined model for p_{back}.

The RMS of the oscillating pressure component (p_{rms}) as a function of flow can be seen in figure 5. The p_{rms} at 1 and 2 cm water depths were lower than for the other water depths.
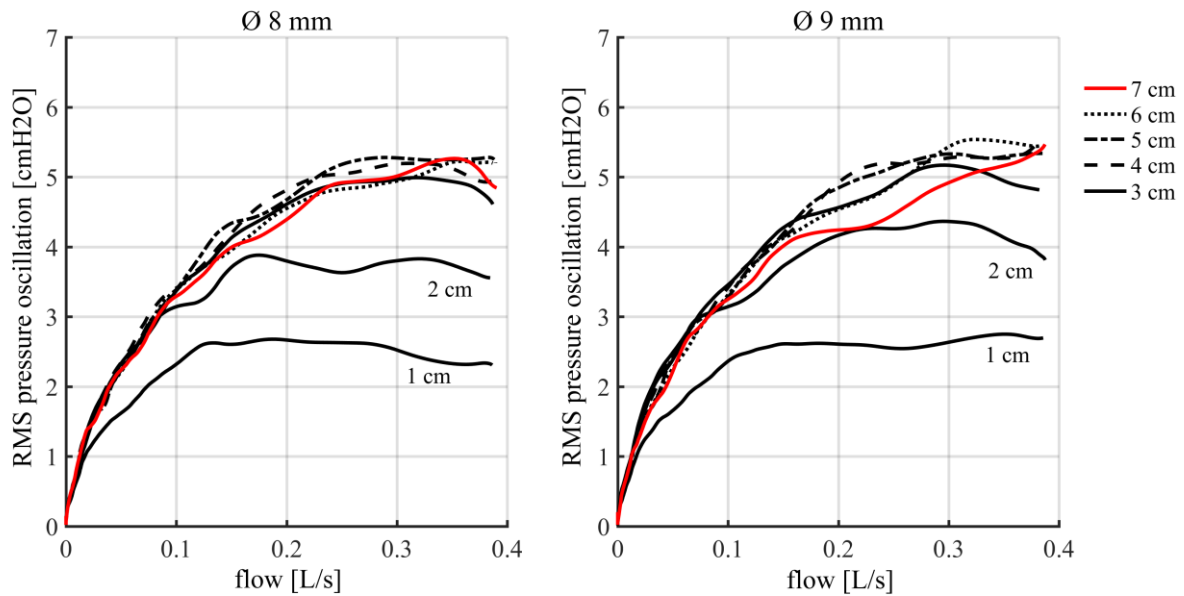

Figure 5. The oscillating component of the pressure as a function of flow for resonance tubes, Ø 8 mm (left) and Ø 9 mm (right) and 26 cm length, in 1-7 cm of water depth. The back cavity volume was 36 cm^3 and angle of tube submersion 45°.

3.2 Experiment 2, bubble types, video recording

The different bubble types are presented in Figures 6 – 8. At 0.005 L/s, the bubbles were produced one by one in a regular pattern; see upper sequences "a" in Figures 6–8. When increasing the flow to 0.013 L/s, the bubble pattern changed to a bimodal version where the bubbles were produced in periodic pairs of two bubbles that merged into a mushroom-like shape; see middle sequences "b" in Figures 6–8. When flow was increased to 0.05 L/s, the bubble pattern turned chaotic and no regularities were visible; see lower sequences "c" in

Figures 6–8. Locations corresponding to sequences a-c are also indicated above the
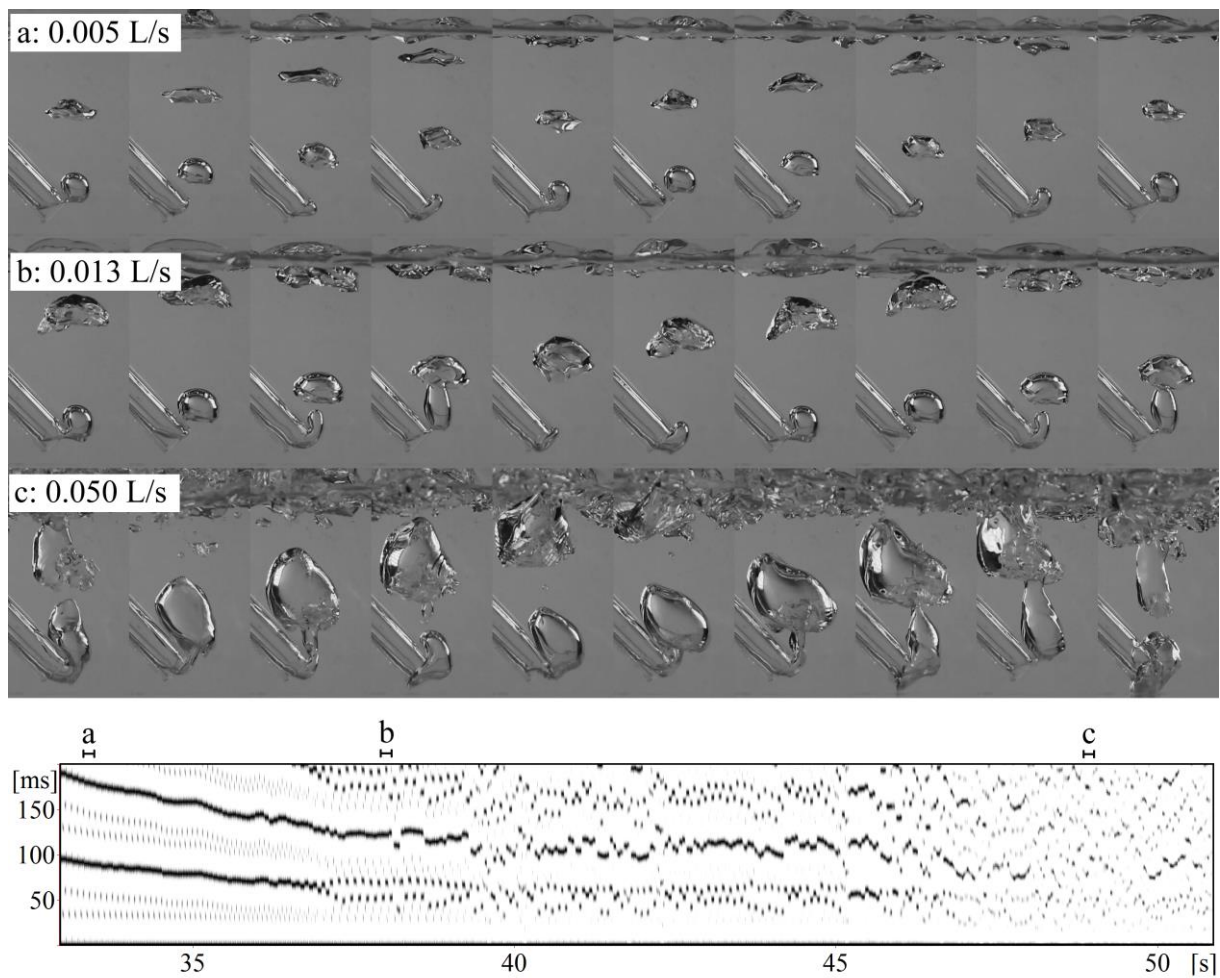correlograms.

Figure 6. Periodic (a), bimodal (b) and chaotic (c) bubble modes at different flows using a Ø 9
mm 26 cm resonance tube submerged 6 cm in water, presented by picture extractions from the
video recording and the corresponding time points in a correlogram of the pressure signal.

Figure 7. Periodic (a), bimodal (b) and chaotic (c) bubble modes at different flows using a Ø 9 mm 26 cm resonance tube submerged 4 cm in water, presented by picture extractions from the video recording and the corresponding time points in a correlogram of the pressure signal.
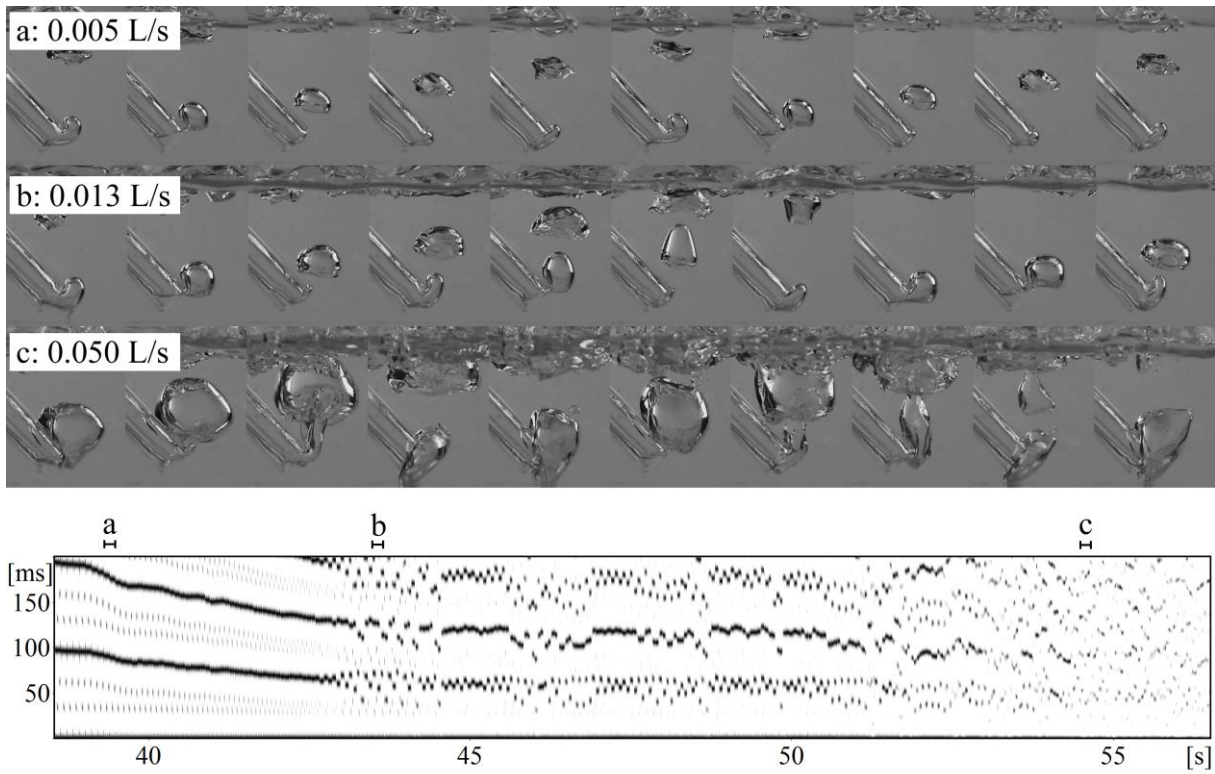
Figure 8. Periodic (a), bimodal (b) and chaotic (c) bubble modes at different flows using a Ø 9 mm 26 cm resonance tube submerged 2 cm in water, presented by picture extractions from the video recording and the corresponding time points in a correlogram of the pressure signal.
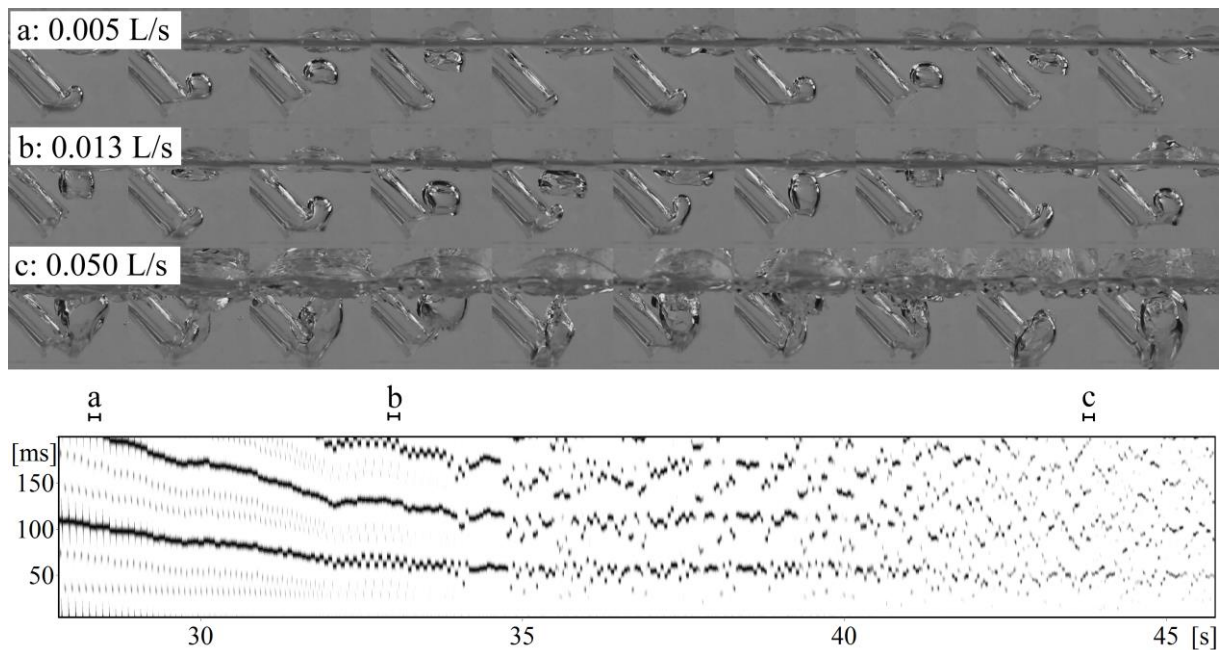
3.3 Experiment 3, bubble types as a function of flow

The shifts between regular, regular with bimodal components, bimodal, bimodal with chaotic components and chaotic bubble types were identified in the correlogram of the p_{back} signal, recall figure 3.

Average flow values for the shifts in bubble mode were determined by visual inspection of correlograms by two raters, table I. Inter and intra rater agreement were calculated using intra class correlation (ICC). The ICC between the raters were ICC = .859 (single measures, confidence interval of 95 % from .834 to .881, F(479) = 13.175, $p < .001$). The intra rater agreement for rater 1 was ICC = .959 (single measures, confidence interval of 95 % from .948

to .968, F(239) = 47.873, p < .001) and for rater 2 ICC = .932 (single measures, confidence interval of 95 % from .913 to .947, F(239) = 28.445, p < .001). Thus, the ICC analyses indicated good to excellent intra and inter rater agreements in all cases [21].

Kruskal-Wallis tests showed that there was a statistically significant difference in airflow at the different shifts in bubble modes, $\chi^2(3)$ = 799.334, p < .001. The mean rank scores for the different shifts were 169.42 for shift 1, 328.62 for shift 2, 591.47 for shift 3 and 832.49 for shift 4. A statistically significant difference between water depths was also found, $\chi^2(2)$ = 12.362, p = .002, with mean rank scores of 490.19 for 2 cm of water depth, 513.27 for 4 cm of water depth and 438.05 for 6 cm of water depth. This showed that the shifts in bubble modes occurred at lower flows at 6 cm of water depth than at 2 cm of water depth. The highest flows required for shifts in bubble modes were detected at 4 cm of water depth. A Mann-Whitney U test showed a statistically significant difference between tube diameters (U = 99152.5, p < .001). Mean rank scores were 447.07 for the Ø 8 mm tube and 513.93 for the Ø 9 mm tube, showing that the shifts in bubble modes occurred at lower airflows for the narrower tube.

PLEASE INSERT TABLE 1 ABOUT HERE

3.4 Experiment 4, bubble frequency and volume as a function of flow

The bubble frequency and volume as functions of flow are shown in Figure 9 and 10, respectively. The bubble frequency was extracted by identifying peaks in the spectra of p_{back}. The bubble frequency was only possible to register reliably up to the shifts to chaotic bubble patterns. The shifts varied between takes, thus the bubble frequency was sometimes detectable for the higher flows and sometimes not. The highest flows enabling measurement of the bubble frequencies differed between the diameters and water depths, as seen in figures 9 and10.
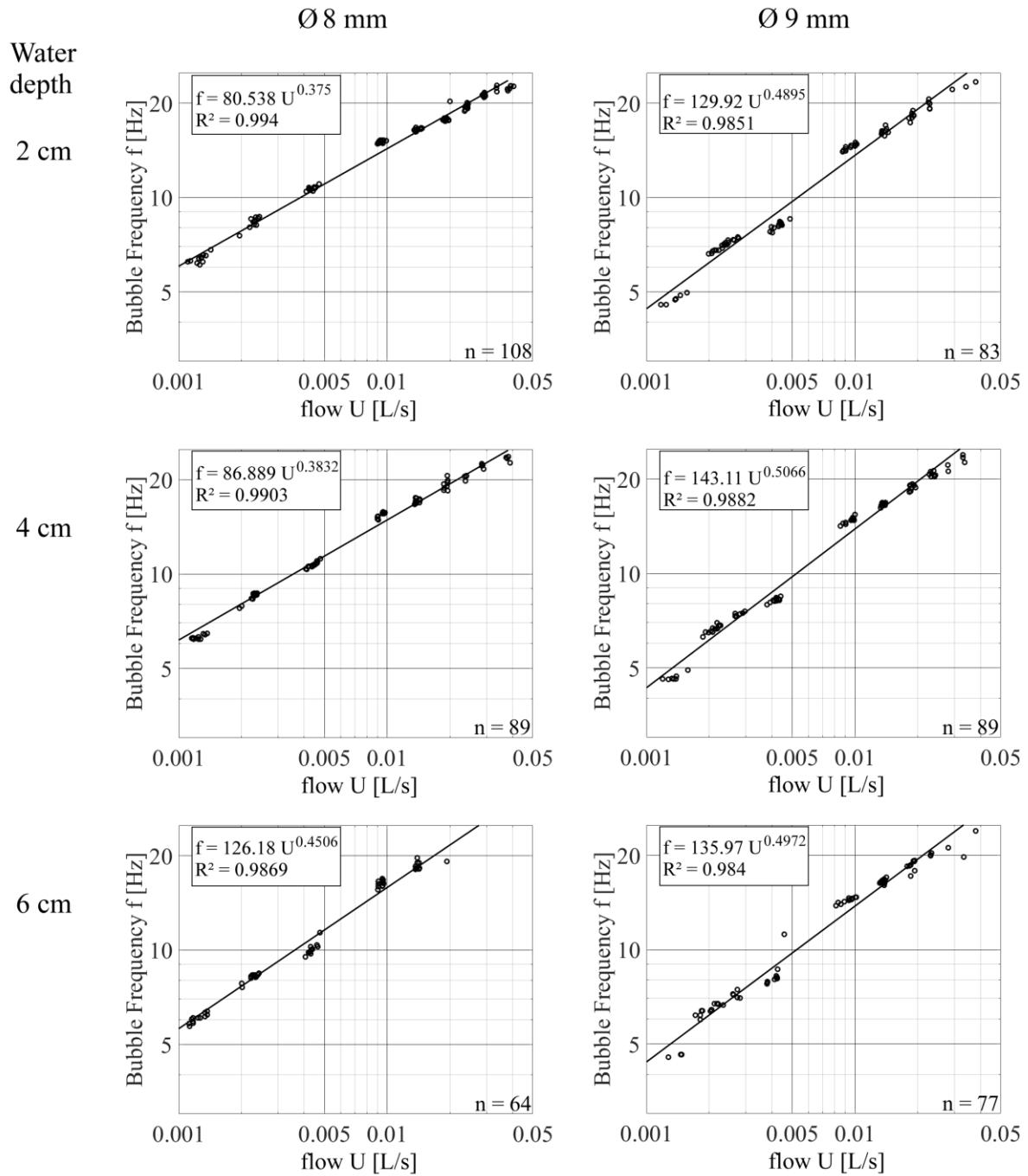
Figure 9. Bubble frequency as a function of flow at three different water depths with an Ø 8 mm (left) and an Ø 9 mm (right), 26 cm long resonance tubes. Back cavity volume was 36 cm^3 and tube angle 45°. Each point represents one measurement. The total amount of points is noted in the lower right corner of the graphs.
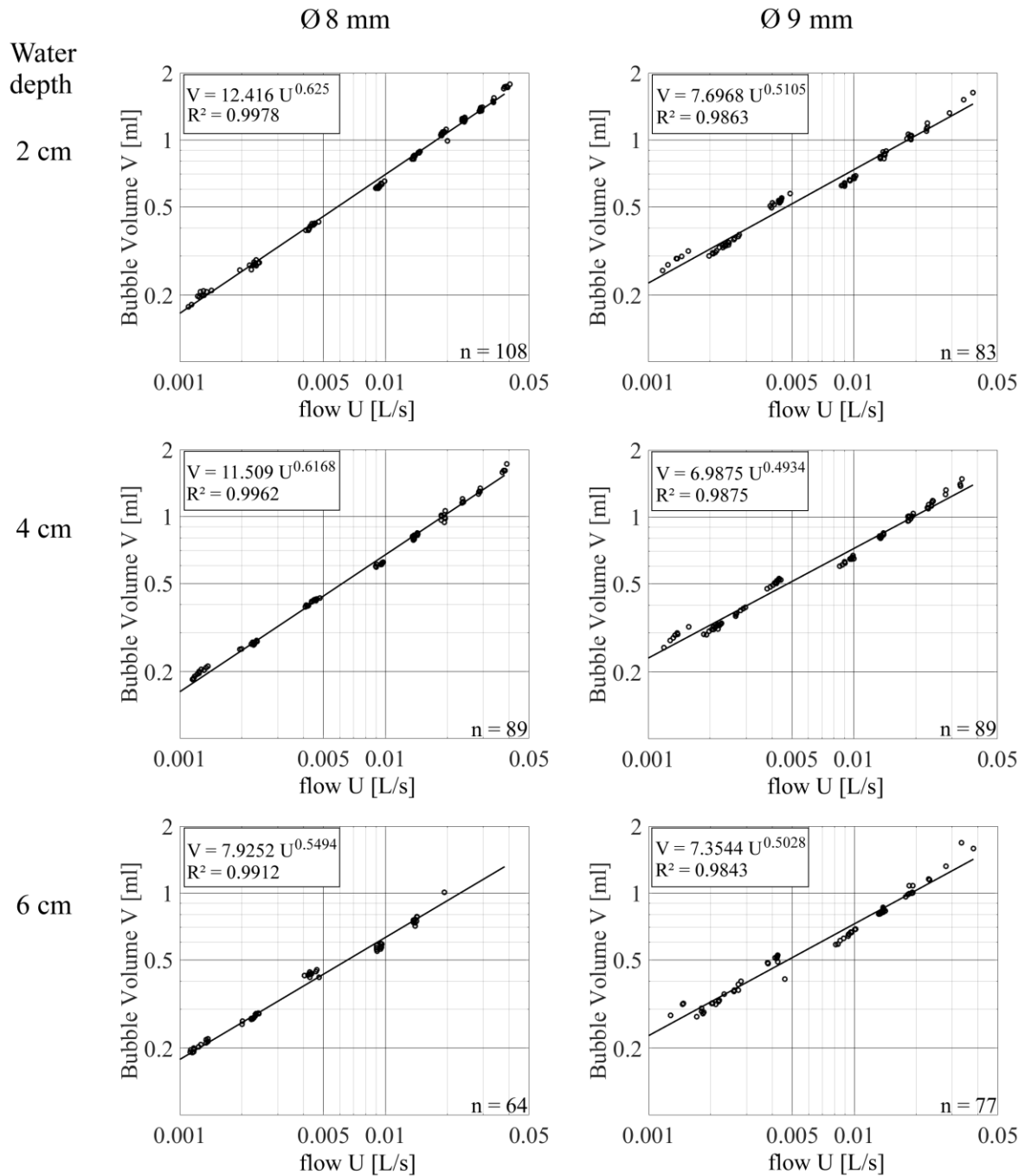
Figure 10. Bubble volume as a function of flow at three different water depths with an Ø 8 mm (left) and Ø 9 mm (right), 26 cm long resonance tubes. The data points were calculated directly from the bubble frequency data in figure 8. Each point represents one measurement. The total amount of points is noted in the lower right corner of the graphs.

3.5 Experiment 5, bubble frequency and volume as a function of back volume

The bubble frequency and volume as functions of back volume can be seen in figures 11 and 12, respectively. Ten different back volumes were set, ranging from 6 to 60 ml in steps of 6 ml. For the higher flow (0.02 L/s) and small back volumes, the bubble patterns varied between bimodal and chaotic, sometimes making detection of bubble frequency impossible. The number of detectable bubble frequencies at different back volumes during 0.02 L/s flow are shown in table II.

A Kruskal-Wallis test showed that changing the back volume had a statistically significant effect on the bubble frequency for the higher flow ($\chi^2(8) = 48.868$, $p < .001$, mean rank scores for the different back volumes: 12 ml = 124.67, 18 ml = 115.86, 24 ml = 104.25, 30 ml = 93.79, 36 ml = 83.88, 42 ml = 67.18, 48 ml = 59.20, 54 ml = 45.50 and 60 ml = 41.75), resulting in lower bubble frequencies at larger back volumes. A similar change in back volume for the lower flow did also result in statistically significant changes in the bubble frequencies, although on a lower significance level (($\chi^2(9) = 17.749$, $p = .038$, mean rank scores for the different back volumes: 6 ml = 120.95, 12 ml = 129.30, 18 ml = 120.60, 24 ml = 105.75, 30 ml = 3.00, 36 ml = 100.15, 42 ml = 91.63, 48 ml = 84.42, 54 ml = 75.95 and 60 ml = 83.25).

Correspondingly, the bubble volumes increased significantly with increasing back volume for both flows ($\chi^2(8) = 48.868$, $p < .001$, for the higher (0.02 L/s) flow, mean rank scores for the different back volumes: 12 ml = 21.33, 18 ml = 30.14, 24 ml = 41.75, 30 ml = 52.21, 36 ml = 62.13, 42 ml = 78.83, 48 ml = 86.80, 54 ml = 100.50 and 60 ml = 104.25, and $\chi^2(9) = 17.749$, $p = .08$ for the lower (0.005 L/s) flow, mean rank scores for the different back volumes: 6 ml = 80.05, 12 ml = 71.70, 18 ml = 80.40, 24 ml = 95.25, 30 ml = 108.00, 36 ml = 100.85, 42 ml = 109.38, 48 ml = 116.57, 54 ml = 125.05 and 60 ml = 117.75).

Mann-Whitney U tests showed that the bubble frequencies were significantly higher for the Ø 8 mm tube than for the Ø 9 mm tube ($U = 8663.0$, $p < .001$, mean rank scores 209.74 for the Ø 8 mm tube and 137.72 for the Ø 9 mm tube), and the bubble volumes were correspondingly smaller for the Ø 8 mm tube than for the Ø 9 mm tube ($U = 7963.0$, $p < .001$, mean rank scores 132.12 for the Ø 8 mm tube and 212.26 for the Ø 9 mm tube), The bubble frequencies and volumes were significantly lower for the lower flow than for the higher flow ($U = 0$, $p < .001$, mean rank scores 100.5 for the 0.005 L/s flow and 273.0 for the 0.02 L/s flow, for both bubble frequencies and volumes)
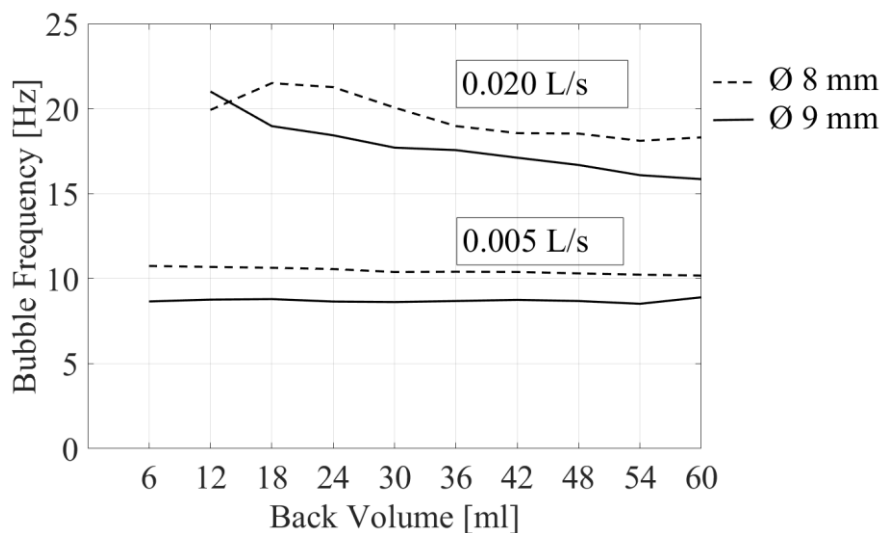

Figure 11. Bubble frequency as a function of back volume at two set flows for two diameter tubes at 2 cm water depth.

Figure 12. Bubble volume as a function of back cavity volume at two set flows for two diameter tubes at 2 cm water depth.
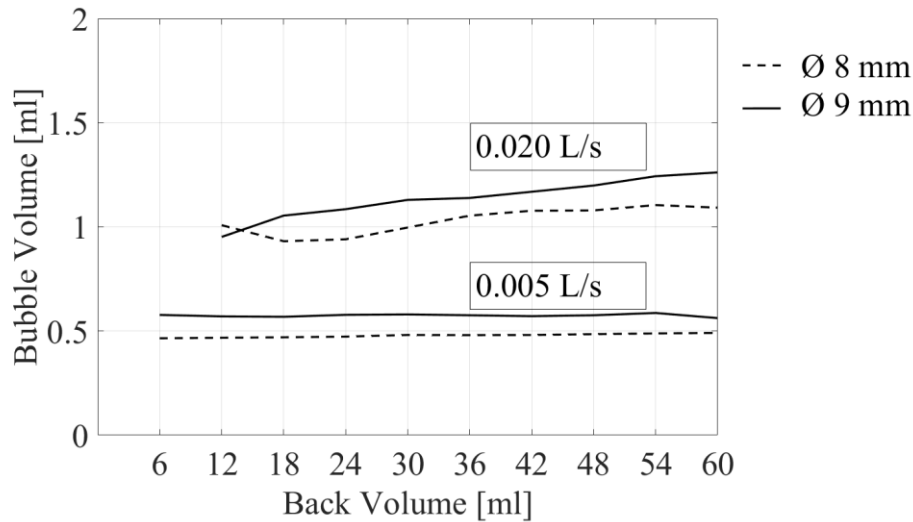
Figure 12. Bubble volume as a function of back cavity volume at two set flows for two diameter tubes at 2 cm water depth.

4. DISCUSSION

The purpose of the present study was to examine the back pressure and bubble formations provided by resonance tubes with tube end in water. In vocal exercises, the back pressure corresponds to the oral pressure. Five experiments were done, using a flow driven vocal tract simulator with a back cavity volume resembling the vocal tract.

The first experiment investigated the flow-pressure relationship for the two diameter tubes, in air and at seven different water depths. The static and oscillating parts of the p_{back} were analyzed separately. The static part of p_{back} was strongly dependent on the water depth and slightly dependent on flow. In practice, this means that the static component of the oral pressure is largely determined by the water depth, and that the subglottal pressure has to overcome that for bubbles to appear. At closer observation, the flow sometimes started slightly below the pressure that the corresponding water depth would induce. This is probably

due to how the water depth was measured. Due to the angle of 45˚, the air column did not reach all the way down to the tube end between bubbles for the lowest flows, which resulted in a lower average pressure during the bubble cycle, than the pressure at the lower end of the tube would provide. However, for higher flows the air column did reach the lower end of the tube for most of the time, resulting in a higher average pressure approximately corresponding to the pressure at the lower end of the tube. This could also be seen in the video recordings in experiment 2 (see the top sequences in figure 6 a-c). The agreement between back pressure and the pressure at the lower end of the tube is coincidental and relies on the angle of approximately 45º. If using a downward (90º) angle of submersion, the model would have to be modified accordingly, because the actual depth for an emitted bubble would be greater than the depth at the tube end, as shown by Amarante Andrade et al [10] in their figure 3.

In addition to the pressure given by the water depths, there was also a small flow resistance in the tubes. The Ø 8 mm tube showed a slightly steeper increase of p_{back} during increasing flow than the Ø 9 mm tube, which would be expected due to the higher flow resistance of the narrower tube. Comparing our experimental data to the model of pressure-flow relationships for tubes in free air [11] showed that our data generated a similar p_{back} as the model. The measured data shows a small but systematic underestimation of the back pressure in our combined model for the tube in water. This underestimation may be explained by the resistance of the extra constriction that appears when there is water in and near the tube end. The difference in resistance between tube diameters of 8 and 9 mm seems to be so small (resulting in a pressure difference of less than 1 cm H_2O), so it might not be of any clinical importance.

In addition to the static component, p_{rms} was quantified using the RMS amplitude of the oscillating component of p_{back}. The oscillating component has earlier been referred to as providing a so called massage effect [2,6,14]. The largest values of p_{rms} were found to plateau around 5-6 cmH$_2$O at high flows, and occurred for water depths 3 to 7 cm. For 2 cm of water

depth, p_{rms} plateaued near 4 cmH$_2$O, and at 1 cm of water depth, it plateaued at around 2.5 cmH$_2$O (recall Figure 5). For all water depths, the p_{rms} decreased towards zero flow. The p_{rms} values were slightly larger for the Ø 9 mm tube than for the Ø 8 mm tube.

The plateauing of p_{rms} is interesting, especially as Simberg and Laine [8] recommend not submerging the tube end deeper than 2 cm whilst keeping a steady phonation. This water depth will provide medium p_{rms}, without a large static p_{back}, as the oscillating part will not change with greater depths than 3 cm. Submerging the tube end beyond 3 cm will not increase p_{rms} considerably, however the static part of the p_{back} will increase with increasing water depth. However, the oscillating component causes the peak vocal tract pressures to be considerably higher than the static pressures. The constant p_{rms} for depths over 3 cm is in line with Guzman et al [13], who found no significant differences in the peak-to-peak amplitudes of the oral pressure modulations for 45 subjects during bubbling at 3 and 10 cm water depth using a 55 cm long silicone tube. This knowledge might be important to consider in the clinical setting.

The second and third experiment focused on bubble formation modes. The formation of bubbles when air is blown into water was studied already in the 1960's and earlier, but to our knowledge this research has not been put in the context of voice training with resonance tube phonation in water. Most of the earlier research was done with a vertical, upward facing tube end, in contrast to the tube phonation where the tube has a downward angle of about 45°. Our research shows however that the formation of bubbles is similar to that of the vertical end, where the bubbles at low flows are emitted one by one in a periodic manner, at medium flows the bubbles are emitted in pairs resulting in a mushroom like shape and at high flows the bubbles are emitted in a chaotic manner [17]. No data on human airflow usage during resonance tube phonation in water seems to be available, so to date it is unclear which bubble mode actually is the most commonly used with patients and whether the patients could use the

bubble mode as a feedback. Granqvist et al [6], figure 2, show a picture of a possible regular to bimodal bubble pattern produced by a participant instructed to perform the exercise in a normal way. This indicates that the participant used a flow resulting in the bimodal region. However, typical airflow usage during resonance tube phonation in water needs to be investigated in future studies.

In experiments 2 and 3 the time between bubbles was studied by means of a correlogram. Extracting the time between bubbles is non-problematic at low flows providing regular bubble formations. Methods used for extracting fundamental frequency can be applied. However, for the bimodal and chaotic regions, the same problem occurs as with voices with a high degree of perturbation in the fundamental frequency. The correlogram presents several candidates for period time, and has a greater time resolution than spectral methods. Thus, the correlogram serves the purpose well of illustrating the periodicity of signals with both regular and irregular period times, such as p_{back}.

In experiment 3 the determination of where the shifts occurred was slightly problematic, as there was a randomness in the appearance of the bimodal and chaotic occurrences (recall figure 3). For example, in the region marked as bimodal, the second candidate would have been expected to be completely smooth if the signal had been perfectly bimodal. However, this is not the case and this type of irregularity is typical for the present data. Nevertheless, we find it worthwhile to attempt to categorize the shifts between bubble modes as presented because the modes seem to appear in all takes although with a random component in how they occur.

Despite the inconsistencies of the system, the reliability between the raters was good [21]. The transitions between bubble modes occurred at slightly lower flows for the narrower tube, although exceptions could be noted in some of the takes. The transitions occurred at the lowest flows at the 6 cm water depth, and at the highest flows at the 4 cm water depth. This

finding indicates that bubble emissions are affected differently at different water depths. In this study, the transitions were only rated at an increasing flow. The shifts may have occurred at slightly different flows if using decreasing flow, due to the chaotic nature of the system. This phenomenon was however not investigated in this paper. The fourth experiment investigated the bubble frequencies and volumes at different airflows. Not surprisingly, the bubble frequency increased with increasing flow, but at a lower rate for high flows. Hence, the volume of the bubbles also increased with increased flow. Only small differences in bubble frequencies could be seen between the different tube diameters and water depths. The bubble frequencies reached 22–23 Hz and 20–22 Hz, with the Ø 8 and Ø 9 mm tube, respectively, for the highest possible flows before entering the chaotic oscillatory modes. The graphs (figures 9 and 10) extend to higher flows than the average points of shift to chaos in experiment 3, which is possible due to the fact that the last points represent the few takes where the shift to chaos had not yet appeared.

The fifth experiment investigated bubble frequencies and volumes at two fixed flows with a varying back volume at 2 cm submersion depth. The results showed that the bubble frequencies decreased with an increasing back volume, especially for the higher flow (Figure 11). This finding could also be relevant in voice therapy, as changes in vocal tract volume have been observed during and after SOVT exercises [19]. It could also be speculated that the degree of glottal adduction may be reflected in the bubble frequency and bubble volume. Less adduction opens the passage to the subglottal tract, and thus the back cavity appears larger.

If the subglottal pressure is kept constant, an increased oral pressure leads to a decreased transglottal pressure. Results from earlier studies suggests that a narrow straw providing a high flow resistance might be useful for example during warm-up for singing or other vocally demanding tasks [1], since it enables the singer to keep a high subglottal pressure combined with a low transglottal pressure. This effect should also be present in tube phonation in water.

The modulation of the oral pressure modulates the vocal fold oscillation [6,22]. If the subglottal pressure is constant, the transglottal pressure oscillation has the same amplitude as the oral pressure variations. If, on the other hand, the subglottal pressure also becomes modulated by the p_{back} of the tube, the transglottal pressure oscillation would be smaller. Horácek et al [23] provide some data from a physical model of the vocal folds and vocal tract during resonance tube phonation in water at 10 cm water depth. In their figure 3b [23], a low frequency pressure oscillation of about 60 ms, presumably related to the reported bubble frequency of 16 Hz, modulates subglottal, transglottal and oral pressure. Thus, the p_{back} oscillations do propagate to the subglottal cavity and it would be reasonable to assume that glottal resistance would affect the extent of subglottal pressure oscillation. It could be speculated that a larger transglottal modulation would be present for pressed voice than for flow phonation. This implies that the resonance tube could potentially be used as a feedback device for adduction. This needs to be investigated further.

The static oral pressure can be controlled for via the water depth. The recommendation of a water depth of 1-2 cm [8] during continuous phonation will provide a relatively low static oral pressure. However, for patients with vocal fold paresis and incomplete closure of the glottis, the same authors recommend short phonations at a greater water depth to resemble pushing exercises[8]. The static part of the p_{back} enables the therapist to have some control over the subglottal pressure that the patient produces.

Some studies have looked at bubble frequencies during resonance tube phonation in water with human subjects. Granqvist et al [6] reported bubble frequencies between 10 and 13 Hz. Wistbacka et al [7] reported bubble frequencies between 14 and 22 Hz. Both studies investigated bubble frequencies at two different immersion depths with two participants, using Ø 9 mm glass tubes of lengths between 26 and 28 cm. Guzman et al [13] reported bubble frequencies between 12 and 32 Hz, with an average of 22 Hz for 45 participants using

a Ø 10 mm, length 55 cm silicone tube at immersion depths 3 and 10 cm. Horácek et al [24] used a Ø 6.8 mm, length 26.4 cm glass tube at three different water depths in order to measure bubble frequencies from spectra of the oral pressure signal. The frequencies reported varied between 15 and 18 Hz. Interestingly, from the pressure spectrum shown in the study for phonating through the tube at 2 cm water depth, the dominant spectral peak of 18 Hz appears to be the second partial of a bimodal spectrum, where the first partial appears near 9 Hz. There might be an inconsistency between different studies whether the terminology "bubble frequency" refers to the actual number of bubbles per second or the number of bubble pairs per second. In all these studies except Guzman et al [13], a lower bubble frequency was associated with larger water depths. None of these four studies measured flow, and according to the present study, differences in flow as well as tube diameter can explain the different bubble frequencies. The results from the present study provide the possibility to estimate flow based on bubble frequency and tube diameter. Transitions to chaotic bubble formation occur at surprisingly low flows. Therefore, in regular and bimodal bubble regimes, the flows during resonance tube phonation in water can be expected to be lower than during normal phonation as well as during tube phonation with the free end in air, as estimated by Titze et al [1]. Previous studies on humans have mainly focused on immediate and short term physiological, perceptual and acoustical effects of tube phonation [1,5,6,7,13,22,25,26]. However, the resonance tube can also be seen as a feedback and control device in voice therapy. The three modes of bubble formation and bubble frequencies can serve as flow feedback. In particular, if the therapeutic goal is to lower the airflow, the patient could be instructed to produce "calm" bubbles, associated with regular or bimodal bubble formations. Using an open bowl encourages the use of a low flow in order to avoid splashing. This highlights a difference between resonance tube phonation in water and the LaxVox technique, in which the bowl is replaced by a water bottle. A closed container allows for the use of a higher flow without

splashing. This indicates that the two methods might be differently suited for different therapy goals.

The tube dimensions recommended by Sovijärvi [4] suggest different tube diameters depending on if the patient is an adult or a child. Tubes for adults are recommended to have a diameter of 9 mm and tubes for children a diameter of 8 mm [4]. However, the physical differences investigated in this study between the two diameters were small, and possibly not clinically important. Sovijärvi further recommends different tube lengths depending on voice category [4]. Possible effects of tube length were not investigated in the present study.

Although differences found between the Ø 8 mm and Ø 9 mm tubes were small, there may be important interaction parameters between the system and the patient within the clinical setting that were not investigated in this study. These parameters could include acoustic interaction with the vocal fold oscillations, perception of sound and the tactile experience by the patients. Thus, several mechanisms have been identified that the voice therapist can take advantage of, in order to provide appropriate visual, perceptual and tactile goals to the patient. These goals may improve reproducibility of the exercise during home practice.

5. CONCLUSIONS

A flow-driven vocal tract simulator was used to obtain information on the physical properties of resonance tubes submerged in water. The results from this study provide information about the static and oscillatory components of back pressure, bubble frequency, volume and mode, as well as how these variables depend on airflow, water depth, tube diameter and back cavity volume. The results provide a scientific ground facilitating further systematic development of SOVT exercises as well as understanding differences between their different types.

Declaration of interest

No conflicts of interest.

REFERENCES

[1] I.R Titze, E. Finnegan, A-M. Laukkanen, S. Jaiswal, Raising lung pressure and pitch in vocal warm-ups: the use of flow-resistant straws, J. Sing. 58 (2002) 329–338.

[2] P. Amarante Andrade, G. Wood, P. Ratcliffe, R Epstein, A. Pijper, J.G Švec, Electroglottographic study of seven semi-occluded exercises: LaxVox, straw, lip-trill, tongue-trill, humming, hand-over-mouth, and tongue-trill combined with hand-over-mouth, J. Voice. 28 (2014) 589–595.

[3] B.H. Story, A-M. Laukkanen, I.R Titze, Acoustic impedance of an artificially lengthened and constricted vocal tract, J. Voice. 14 (2000) 455–469.

[4] A. Sovijärvi, Die Bestimmung der Stimmkategorien mittels Resonanzröhren. [Voice classification according to resonance tubes]. In: Fifth International Congress of Phonetic Sciences (1965). Basel, NY: Karger.

[5] L. Enflo, J. Sundberg, C. Romedahl, A. McAllister, Effects on vocal fold collision and phonation threshold pressure of resonance tube phonation with tube end in water. J. Speech. Hear. Res. 53 (2013) 1530–1538.

[6] S. Granqvist, S. Simberg, S. Hertegård, S. Holmqvist, H. Larsson, P-Å. Lindestad, M. Södersten, B. Hammarberg, Resonance tube phonation in water: high-speed imaging, electroglottographic and oral pressure observations of vocal fold vibrations – a pilot study. Logoped. Phoniatr. Vocol. 40 (2015) 113–21.

[7] G. Wistbacka, J. Sundberg, S. Simberg, Vertical laryngeal position and oral pressure variations during resonance tube phonation in water and in air. A pilot study, Logoped. Phoniatr. Vocol. 41 (2016) 117–23.

[8] S. Simberg, A. Laine, The resonance tube method in voice therapy: description and practical implementations, Logoped. Phoniatr. Vocol. 32 (2007) 165–170.

[9] S. M. Paes, F. Zambon, R. Yamasaki, S. Simberg, M. Behlau, Immediate effects of the Finnish resonance tube method on behavioural dysphonia, J. Voice. 27 (2013) 717–722.

[10] P. Amarante Andrade, G. Wistbacka, H. Larsson, M. Södersten, B. Hammarberg, S. Simberg, J.G Švec, S. Granqvist, The flow and pressure relationships in different tubes commonly used for semi-occluded vocal tract exercises, J. Voice. 30 (2016) 36–41.

[11] S.L. Smith, I.R. Titze, Characterization of flow-resistant tubes used for semi-occluded vocal tract voice training and therapy. J. Voice. (2016) [Epub 2016 Apr 28]; In press.

[12] M. Sihvo, I. Denizoglu, LaxVox Voice Therapy Technique. Downloadable handouts. Available at www.laxvox.com.

[13] M. Guzman, C. Castro, S. Madrid, C. Olavarria, M. Leiva, D. Muñoz, E. Jaramillo, A-M. Laukkanen, Air pressure and contact quotient measures during different semioccluded postures in subjects with different voice conditions. J. Voice. 2016;[Epub 2015 Oct 29]; In press.

[14] V. Radolf, A-M. Laukkanen, J. Horácek, J. Vesely, D. Liu, In vivo measurements of air pressure, vocal folds vibration and acoustic characteristics of phonation into a straw and a resonance tube used in vocal exercising, Proceedings of the 19th International Conference Engineering Mechanics, Czech Republic. (2013) 478–483.

[15] J. Ramlakhan, R. Mudde, M. Oosterbaan-Beks, B. Goes-de Graaff, J.W. Arendse, Bubbling therapy, Book of Abstracts, Pan European Voice Conference, Prague, Czech Republic. (2013) 195–196.

[16] V. Radolf, A-M. Laukkanen, J. Horácek, D. Liu, Air-pressure, vocal fold vibration and acoustic characteristics of phonation during vocal exercising. Part 1: Measurement in vivo, Engineering Mechanics. 21 (2014) 53–59.

[17] L. Davidson, E.H. JR. Amick, Formation of gas bubbles at horizontal orifices. A.I.Ch.E. J. 2 (1956) 337–342.

[18] A. Tufaile, J.C. Sartorelli, Chaotic behavior in bubble formation dynamics. Physica A. 275 (2000) 336–346.

[19] T. Vampola, A-M. Laukkanen, J. Horácek, J.G Švec, Vocal tract changes caused by phonation into a tube: a case study using computer tomography and finite-element modeling. J. Acoust. Soc. Am. 129 (2011) 310–315.

[20] S. Granqvist, B. Hammarberg, The correlogram: A visual display of periodicity. J. Acoust. Soc. Am. 114 (2003) 2934–2945.

[21] D.V. Cicchetti, Guidelines, criteria, and rules of thumb for evaluating normed and standardized assessment instruments in psychology, Psychological Assess. 6 (1994) 284–290

[22] M. Guzman, A-M. Laukkanen, L. Traser, A. Geneid, B. Richter, D. Muñoz, M. Echternach, The influence of water resistance therapy on vocal fold vibration: a high-speed digital imaging study. Logoped. Phoniatr. Vocol. (2016) [Epub 2016 Aug 2] In press.

[23] J. Horácek, V. Radolf, V. Bula, A-M. Laukkanen. Air-pressure, vocal folds vibration and acoustic characteristics of phonation during vocal exercising. Part 2: Measurement on a physical model. Engineering Mechanics. 21 (2014) 193–200.

[24] J. Horácek, V. Radolf, V. Bula, J. Veselý, A-M. Laukkanen. Experimental investigation of air pressure and acoustic characteristics of human voice. Part 1: Measurement in vivo. In J.Náprstek & C. Fischer (Eds.), Engineering Mechanics 2012. Proceedings of the 18th International Conference, Svratka, Czech Republic. Institute of Theoretical and Applied Mechanics, Academy of Sciences of the Czech Republic. Prague (2012) 403-417.

[25] M. Guzman, D. Higueras, C. Fincheira, D. Muñoz, C. Guajardo, J. Dowdall, Immediate acoustic effects of straw phonation exercises in subjects with dysphonic voices. Logoped. Phoniatr. Vocol, 38 (2013) 35–45.

[26] M. Guzman, G. Miranda, C. Olavarria, S. Madrid, D. Muñoz, M. Leiva, L. Lopez, C. Bortnem, Computerized tomography measures during and after artificial lengthening of the vocal tract in subjects with voice disorders. J. Voice. 31 (2017) 124.e1 – 124.e10.

Table I. Median and inter quartile range of the airflow at points of shift in bubble modes from experiment 3, determined visually by two raters using correlograms. The ratings were done twice by both raters on 10 takes per task. Hence, all values are based on 4x10 flow values. The numbering of the shifts correspond to those in figure 3.

Diameter [mm]	Water depth [cm]	Flow at bubble mode shifts [L/s]			
		Shift 1 Regular-regular with bimodal comp	Shift 2 Regular with bimodal components-bimodal	Shift 3 Bimodal-bimodal with chaotic components	Shift 4 Bimodal with chaotic components - chaos
8	2	0.0082 (0.0076-0.0084)	0.0119 (0.0105-0.0131)	0.0180 (0.0169-0.0194)	0.0297 (0.0280-0.0369)
	4	0.0097 (0.0089-0.0100)	0.0100 (0.0098-0.0102)	0.0193 (0.0180-0.0197)	0.0274 (0.0250-0.0325)
	6	0.0089 (0.0087-0.0092)	0.0094 (0.0091-0.0096)	0.0117 (0.0111-0.0130)	0.0247 (0.0220-0.0299)
9	2	0.0081 (0.0076-0.0089)	0.0127 (0.0118-0.0145)	0.0180 (0.0170-0.0196)	0.0253 (0.0233-0.0290)
	4	0.0110 (0.0105-0.0116)	0.0114 (0.0110-0.0122)	0.0186 (0.0179-0.0206)	0.0259 (0.0235-0.0297)
	6	0.0099 (0.0096-0.0105)	0.0110 (0.0106-0.0117)	0.0160 (0.0153-0.0184)	0.0269 (0.0236-0.0321)

Table II. The total number of detectable bubble frequency values at different back volumes at set flow 0.02 L/s.

Tube diameter [mm]	8	9
Back Volume [ml]		
6	0	0
12	2	1
18	2	5
24	6	10
30	9	10
36	10	10
42	10	10
48	10	10
54	10	10
60	10	10